Effect of slag and fly ash on Laboratory NDT measurements for long curing period

Gayelle FAHED [1,2], *Stéphanie BONNET*[1], *Anthony SOIVE*[2]

[1] *Nantes Université, Ecole Centrale Nantes, CNRS, GeM, UMR 6183 F-44600 Saint-Nazaire, France*

[2] *GeoCoD Research Team, Cerema, 13593 Aix in Provence cedex3, France*

Key-words : Slag, Fly Ash, curing period, NDT, Electrical resistivity, Dynamic young modulus.

I. Introduction

Concrete is a widely-used construction material due to its strength, durability, and affordability. However, concerns about the environmental impact of cement production have highlighted the need for low-carbon alternatives such as supplementary cementitious materials (SCMs). To ensure the efficacy and durability of these materials, more research is needed on their microstructure and physicochemical properties throughout the lifespan of the concrete.

Non-destructive testing methods have gained popularity in civil engineering materials research for their ability to assess the properties of materials without altering or damaging them. In this study, we explore the use of laboratory NDT measurement: the dynamic Young's modulus by grindosonic apparatus and apparent electrical resistivity by Wenner apparatus as non-destructive auscultation methods to investigate in saturated condition the influence of slag and fly ash on the modification of low-carbon mortar microstructure.

The apparent resistivity as well as the dynamic young modulus of cement paste or concrete are closely related to the degree of hydration and the microstructure of the material. The apparent resistivity is related to the capillary pore size distribution and interconnection. A finer pore network with less connectivity leads to lower permeability, equating to higher resistivity (Cheytani and Chan, 2021).The size and pore structure are determined by factors such as cement type, water-cement ratio (w/c), pozzolanic admixtures and the degree of hydration of the concrete (Meddah and Tagnit-Hamou, 2009). The young modulus is affected by the stiffness and bonding characteristics of the different phases. Moreover, in concrete, the electrical current is carried by the dissolved charged ions flowing through the pore solution (Sengul and E. Gjørv, 2009) so the electrical resistivity is also affected by the multi-ionic composition of the poral solution depending on the binder and its associated hydrates.

It has been shown that the use of pozzolanic materials refines the pore structure (Meddah and Tagnit-Hamou, 2009). It is a well-known fact that the reaction of fly ash in concrete, only starts significantly after one or more weeks. Until this period the fly ash behaves more or less as an inert material, which only serves as a precipitation nucleus for $Ca(OH)_2$ and C-S-H gel originating from the cement hydration. After the initiation of the pozzolanic reaction of the fly ash, the cement paste will become increasingly denser(Fraay et al., 1989).

In comparison to Portland cement, some authors emphasize that the inclusion of slag causes a denser microstructure, finer-pored and less permeable (Baroghel-Bouny, 2005; Ben Fraj et al., 2019; Teng et al., 2013) which affects largely the transport properties of concrete. At early ages, the

addition of fly ash or slag can reduce the strength of the mortar due to slower early-age hydration of the cement. However, at later ages, the pozzolanic reaction with the cement can lead to additional strength gain and improved durability.
The originality of this study lies in its focus on the evolution of the modulus and resistivity over an extended curing period of 450 days, an area which has not been sparsely explored in literature.

II. Materials and methods

Formulation of mortar

Our study is carried on three mortar compositions. M100 is the standard reference mortar of CEM1 concrete with only portland cement. M35-65S denote for the composition of which 65% of mass of binder is substituted with blast furnance slag and M70-30FA includes 30% Fly Ash. The formulations have been prepared according to the standard NF-EN 196-1(AFNOR, 2016) with a water to binder ratio equal 0.5.

Table 1: ***Mortar mass composition per mold.***

Reference	Mixtures proportions (g).				
	Cement	**Slag**	**Fly Ash**	**Sand**	**Water**
M100	450	-	-	1350	225
M35-65S	158	292	-	1350	225
M70-30FA	315	-	135	1350	225

Methods and instruments

- *Dynamic Young Modulus*

The dynamic modulus E_{dyn} is determined using Impulse Excitation Technique (Grindo Sonic) according to NF EN 12680-1(AFNOR, 2007, pp. 12680–1)The test is performed by placing a small handheld instrument on the surface of the concrete and striking it with a small hammer. The resulting sound wave generated by the impact is picked up by the instrument and is used to calculate the dynamic young modulus of the mortar.

- *Apparent electrical resistivity*

The apparent surface electrical resistivity was measured according to ("NF EN 12390-19," 2021) by the four-point Wenner probe. The resistivity of concrete is measured by creating an electrical current between two outer electrodes and then measuring the voltage between two inner electrodes that are aligned with the outer ones. The 4 electrodes are linearly arranged and spaced at a constant distance of 4 cm.

Measurements were initiated seven days after casting, and were conducted at different intervals during the curing period for the same 4*4*16 cm 6 prisms.

III. Results and discussion

Figure 1, presents the variation of the dynamic young modulus function of the curing time. The mean value of 3 measurements is represented and the error bars correspond to the standard deviations. The highest value of dynamic Young's modulus was obtained for the reference mortar, whereas the slag showed the highest evolution from zero to 450 days. The rate of increase varied among different compositions. M100 exhibited a minor increase during the first 28 days, followed

by stabilization. On the other hand, compositions with SCM's showed a sharp increase during the initial 90 days, resulting in a substantial variation, and then a more gradual increase until approximately 150 days. Additionally, the three compositions displayed consistent dynamic Young's modulus values after 150 days of curing.

The graph of dynamic Young's modulus was observed to be influenced by the process of hydration, which stimulates the formation of various hydrates with distinct elastic properties and the development of CSH. As CSH forms inside the pores, the material's strength increases progressively. The delayed effect of hydration on the delayed increase of the Young's modulus was prominently observed in slag and fly ash mixtures (Meddah and Tagnit-Hamou, 2009).

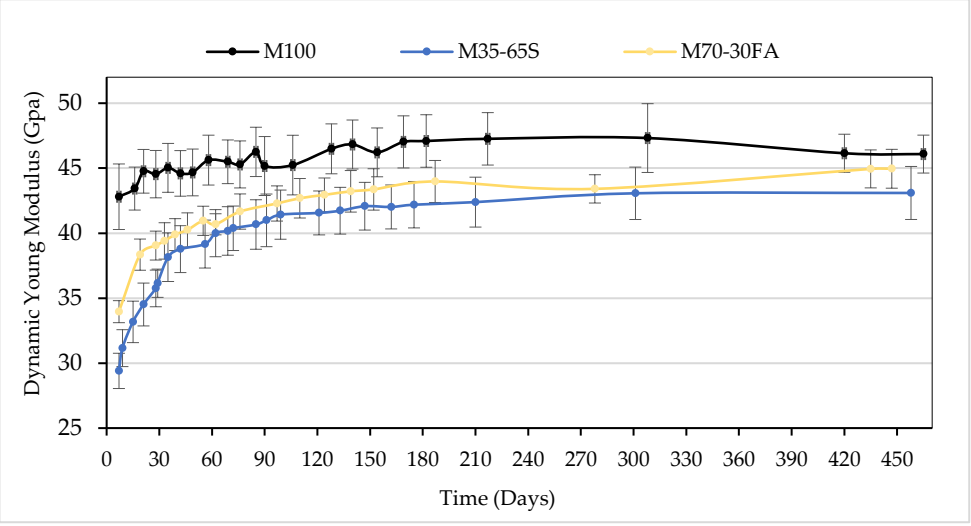

Figure 1:*Dynamic young modulus E_{dyn}.*

Figure 2, presents the variation of the apparent electrical resistivity function of curing time. The mean value of 6 measurements is represented and the error bars correspond to the standard deviations. The apparent resistivity increases over time for all samples due to cement hydration and to the progressive hardening of mortar. This is verified by the tendency to reduce the interconnected pore network of the mortar over time, contributing to reduce the conductivity of the mortar, in agreement with other studies (Medeiros-Junior and Lima, 2016; Presuel-Moreno et al., 2013). The reference mortar showed an initial resistivity of around 220 Ωm, which increased to 450 Ωm within 28 days, and then stabilized at approximately 500 Ωm. However, the presence of SCMs altered the resistivity behavior, with M35-65S taking longer to stabilize and exceeding the 90-day timeframe for delayed hydration. The apparent resistivity increases for fly ash mortar was very slow within the first 50 days, ranging from 330 to 570 Ωm, but showed a sharp rise to 2500 Ωm within the next 150 days, followed by stabilization. The pozzolanic reaction of the fly ash took time to be initiated but once started the microstructure became significantly denser(Fraay et al., 1989).

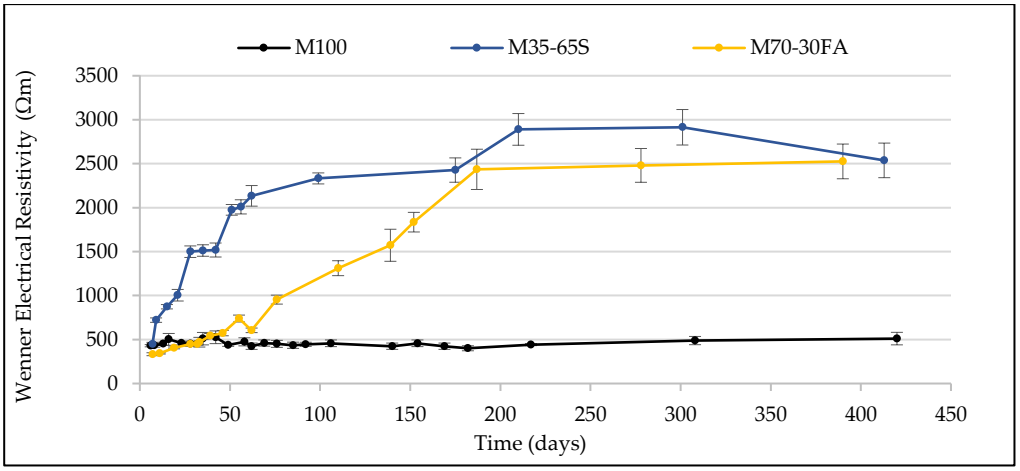

Figure 2: ***Wenner electrical resistivity*** R_{elec}.

Figure 3, presents the relative dynamic young modulus and resistivity to the value obtained at 7 days. The results indicate that the fly ash mortar exhibited the highest increase in relative resistivity, reaching 7.5 times the resistivity obtained at 7 days, followed by the slag composition. While for the dynamic young modulus the composition with slag exhibited the highest augmentation. For M100 there approximately no relative variation since there are no delayed effect beyond 28 days. However, it should be noted that the highest values of resistivity are obtained for the slag incorporated mortar, as shown in **Figure 2**.

At the 450-day mark, the samples with slag and fly ash exhibit diminished Young's modulus values compared to the reference sample. Concurrently, a substantial elevation in resistivity is observed when compared to the reference sample. This observation, despite implying a more refined microstructure in M35-65S and M70-30FA, underscores the significant influence of pore solution composition (ionic activity) and porosity on resistivity. Parallel measurements of compressive strength for these same compositions also revealed elevated strength in mortars with slag and fly ash, which aligns with the resistivity observations.

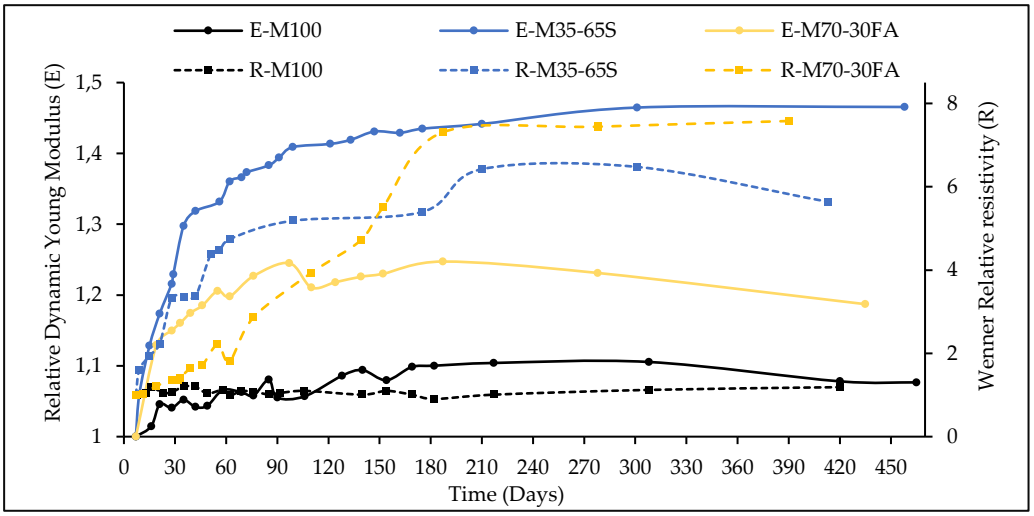

Figure 3: ***Relative value*** E_{dyn} ***and*** R_{elec} ***to the obtained value at 7 days .***

IV. Conclusion

The results showed that apparent electrical resistivity varies along the hydration process, with an increase observed as the pore refinement of the structure improves. The relationship between resistivity and microstructure was confirmed, with a finer pore network leading to lower permeability and higher resistivity. However, further tests such as water porosity, gas permeability, and mercury intrusion porosity are necessary to gain a more comprehensive understanding of variations observed with pozzolanic admixtures. Additionally, it is important to note that other factors such as chemical contaminants can also affect the values of resistivity for mortar. Overall, the results demonstrate the potential of NDT methods in assessing microstructural changes and the evolution of pore solution content in cement-based materials, particularly in evaluating the effects of SCM incorporation on mortar properties.

REFERENCES

AFNOR, N., 2016. NF-EN 196-1 Méthodes d'essais des ciments-Partie1: Détermination des résistances.

AFNOR, N., 2007. NF EN 12680-1: Méthodes d'essais pour produits réfractaires.

Baroghel-Bouny, V., 2005. Which toolkit for durability evaluation as regards chloride ingress into concrete? Part II: Development of a performance approach based on durability indicators and monitoring parameters, in: Third International RILEM Workshop on Testing and Modelling Chloride Ingress into Concrete. RILEM Publications SARL, Madrid, Spain. https://doi.org/10.1617/2912143578.009

Ben Fraj, A., Bonnet, S., Leklou, N., Khelidj, A., 2019. Investigating the early-age diffusion of chloride ions in hardening slag-blended mortars on the light of their hydration progress. CBM, 225, 485–495. https://doi.org/10.1016/j.conbuildmat.2019.07.185

Cheytani, M., Chan, S.L.I., 2021. The applicability of the Wenner method for resistivity measurement of concrete in atmospheric conditions. Case Studies in Construction Materials 15, e00663. https://doi.org/10.1016/j.cscm.2021.e00663

De Belie, N., Soutsos, M., Gruyaert, E. (Eds.), 2018. Properties of Fresh and Hardened Concrete Containing Supplementary Cementitious Materials: State-of-the-Art Report of the RILEM Technical Committee 238-SCM, Working Group 4, RILEM State-of-the-Art Reports. https://doi.org/10.1007/978-3-319-70606-1

Fraay, A.L.A., Bijen, J.M., de Haan, Y.M., 1989. The reaction of fly ash in concrete a critical examination. Cement and Concrete Research 19, 235–246. https://doi.org/10.1016/0008-8846(89)90088-4

Juenger, M.C.G., Siddique, R., 2015. Recent advances in understanding the role of supplementary cementitious materials in concrete. CCR 78, 71–80. https://doi.org/10.1016/j.cemconres.2015.03.018

Meddah, S., Tagnit-Hamou, A., 2009. Pore Structure of Concrete with Mineral Admixtures and its Effect on Self-desiccation Shrinkage. ACI Materials Journal V. 106, 241–250.

Medeiros-Junior, R.A., Lima, M.G., 2016. Electrical resistivity of unsaturated concrete using different types of cement. CBM 107, 11–16. https://doi.org/10.1016/j.conbuildmat.2015.12.168

NF EN 12390-19, 2021.

Presuel-Moreno, F., Wu, Y.-Y., Liu, Y., 2013. Effect of curing regime on concrete resistivity and aging factor over time. CBM 48, 874–882. https://doi.org/10.1016/j.conbuildmat.2013.07.094

Sengul, O., E. Gjørv, O., 2009. Effect of Embedded Steel on Electrical Resistivity Measurements on Concrete Structures - ProQuest. ACI Materials Journal.

Teng, S., Lim, T.Y.D., Sabet Divsholi, B., 2013. Durability and mechanical properties of high strength concrete incorporating ultra fine Ground Granulated Blast-furnace Slag. CBM, Special Section on Recycling Wastes for Use as Construction Materials 40, 875–881. https://doi.org/10.1016/j.conbuildmat.2012.11.052